Calculations of current in the cotunneling regime using Lindblad equations

Kian Maleki
Department of Physics and Astronomy, University of Iowa, Iowa City, Iowa 52242, USA

Michael E. Flatté
Department of Physics and Astronomy, University of Iowa, Iowa City, Iowa 52242, USA and
Department of Applied Physics and Science Education,
Eindhoven University of Technology, 5600 MB Eindhoven, The Netherlands

(Dated: September 3, 2025)

Transport through zero-dimensional states in a tunneling barrier can occur via co-tunneling, wherein a carrier occupying a state outside the range of energies between the chemical potentials of the two leads hops to a lead, and within the brief time permitted by the energy-time uncertainty relationship the occupancy is replenished from the other lead. Here, we calculate the current in such junctions using a Lindblad formalism within the Markovian approximation. We consider transport in the Coulomb blockade regime with spin-polarized leads and a magnetic field smaller than the coercive field of either lead. Dependences on magnetic field and lead spin polarization of the spin blockade, decoherence, and spin lifetime of the subsystems of this model are calculated.

I. INTRODUCTION

Spin transport electronics (spintronics) focuses on the combined electrical and magnetic behavior of the transport of spin, especially through nanoscale geometries[1–4]. Some spintronic devices, especially magnetic disk read heads and magnetic random access memory, have made the transition to technologies[5]. Although considerable current research now focuses on the transport of spin through magnetic insulators[6], *i.e.* in the absence of charge transport, there are a range of situations where spintronic properties combined with the spatial motion of electrons remains of interest, such as a recent focus on antiferromagnetic tunnel junctions[7–10]. Another example is the magnetoresistance of transport through localized states, both with nonmagnetic and magnetic leads, with a focus on spin blockade[11]. This phenomenon was extensively explored in combination with controversies over so-called three-terminal Hanle measurements[12, 13], providing alternate interpretations for some experiments reporting spin injection into semiconductors and other nonmagnetic conductive regions[14]. The associated features of these phenomena, characterized by spin blockage (and its release) and the interaction with hyperfine fields[15–18], have provided possible applications to room-temperature quantum sensors[19]. Furthermore the demonstration of these effects in the single-spin limit[20] suggests a pathway to efficient qubit initialization[21] and coherent manipulation for quantum information processing[22].

The calculations of these effects have focused on sequential tunneling, whether in the resonant or nonresonant regime. In these models the carrier (electron or hole) moves from one lead to the defect state and then to the other lead, with energy conservation anticipated to be enforced by the thermalization of excess energy into phonons through the hopping process. However there are scenarios where the transport can occur via an alternate pathway wherein the initial hopping process originates from a carrier in a defect state outside of the "bias window", *i.e.* the range of energies between the chemical potentials of the two leads, and concludes with that carrier in a lead. This process is briefly permitted according to the energy-time uncertainty relationship, and if the defect occupancy is replenished from the other lead then this "cotunneling" process contributes to the current[23–26].

Here we calculate this cotunneling process for spin transport within the Markovian approximation using the Lindblad formalism. This model captures this phenomenon with a few parameters describing rates to and from the defect state, rates of precession, and decoherence times on the defect site. Our interest in this formalism lies in the current itself and how both cotunneling and current are affected by applying a magnetic field to the defect and the magnetized contacts. We focus on the weak cotunneling regime, where the intrinsic relaxation rate of the defect is much smaller than I/e [27]. Subsequently, we examine the effect of the magnetic field and magnetized contacts, which can block or allow the polarized current, thereby providing control over the polarized current. We anticipate that this formalism should be of use to describe cotunneling in zero-dimensional tunnel junctions and similar quantum systems [28].

II. THEORY

The system of interest is a localized state, perhaps associated with a quantum dot or defect, between two metallic leads with the chemical potentials μ_l and μ_r at the left and right contacts respectively. The Hamiltonian of this system is

$$\begin{aligned} \mathcal{H} &= \mathcal{H}_o + V \\ \mathcal{H}_o &= \mathcal{H}_L + \mathcal{H}_S \end{aligned} \tag{1}$$

with

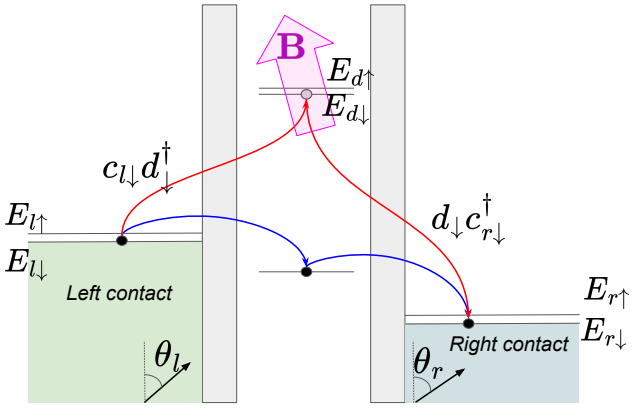

FIG. 1. System schematic. The electrical contacts are spin polarized, and the spin center energy level is located outside of the bias window. Red arrows indicate classically-prohibited cotunneling. Blue arrows indicate sequential tunneling.

$$\begin{aligned}
\mathcal{H}_L &= \sum_{m=l,r}\sum_{k}\epsilon_k c^{\dagger}_{mk}c_{mk}\\
\mathcal{H}_S &= \sum_{n}^{N}\epsilon_p d^{\dagger}_p d_p\\
V &= \sum_{m=l,r}(D_m + D^{\dagger}_m)\\
D_m &= \sum_{k,n}^{N} T_{mkn}c^{\dagger}_{mk}d_n
\end{aligned} \tag{2}$$

In the above equations, $\mathcal{H}_L$ and $\mathcal{H}_S$ represent the leads and the zero-dimensional state, respectively. The effect of the polarized contacts is accounted for by ϵ_k, where k is a quantum number referring to the wave number of the carriers. N denotes the total number of zero-dimensional states. The perturbation V drives the tunneling process. T_{mkn} is the hopping parameter between the contact and the state within the barrier. Figure 1 illustrates the system.

The state of the system is described using the density matrix

$$\begin{aligned}
\rho_o &= Z^{-1}exp\Big(-K/k_BT\Big),\\
\rho(t) &= exp\Big(-i\mathcal{H}t\Big)\,\rho_o\, exp\Big(i\mathcal{H}t\Big),
\end{aligned} \tag{3}$$

with

$$\begin{aligned}
K &= \mathcal{H}_o - \sum_{m=l,r}\mu_m N_m,\\
N_m &= \sum_k c^{\dagger}_{mk}c_{mk}.
\end{aligned} \tag{4}$$

The current operator is

$$\hat{I}_m = \frac{ei}{\hbar}[V, N_m] = \frac{ei}{\hbar}\Big(D^{\dagger}_m - D_m\Big). \tag{5}$$

The average current can be calculated using the following equations:

$$\begin{aligned}
I &\equiv I_2 = -I_1,\\
I_m &= Tr\Big(\rho_o \hat{I}_m\Big).
\end{aligned} \tag{6}$$

The time evolution of the current operator is determined from

$$U(t) = Texp\Big(-i\int_{-\infty}^{t} dt' V(t')\Big). \tag{7}$$

To calculate the current $U(t)$ is typically expanded using perturbation theory.

We employ the Markovian approximation and solve the evolution of the density matrix within the Lindblad formalism. Within the Markovian approximation the current can be found using the steady-state density matrix, ρ^{ss}:

$$I_m = Tr\Big(\rho^{ss}\hat{I}_m\Big), \tag{8}$$

where ρ^{ss} is the steady-state density matrix, defined as

$$\rho^{ss} = \lim_{t\to\infty}\rho(t). \tag{9}$$

Here, we consider spin-dependent transport involving one spin center. The basis can be constructed from states of definite particle number and spin. These six states are $|(n_l+1)n_d n_r\rangle_{\uparrow}$, $|n_l(n_d+1)n_r\rangle_{\uparrow}$, and $|n_l n_d(n_r+1)\rangle_{\uparrow}$, as well as their spin-down counterparts.

The Hamiltonian that governs the coherent evolution of the system with a polarized contact and one spin center, for a fixed wave number (k), is

$$\begin{pmatrix} E_{l\uparrow}+g_lP_{lz} & g_l\Big(P_{lx}+iP_{ly}\Big) & h_{ld}^{\uparrow} & 0 & 0 & 0 \\ & E_{l\downarrow}-g_lP_{lz} & 0 & h_{ld}^{\downarrow} & 0 & 0 \\ & & E_{d\uparrow}=E_d+g_dBz & g_d\Big(B_x+iB_y\Big) & h_{dr}^{\uparrow} & 0 \\ & & & E_{d\downarrow}=E_d-g_dBz & 0 & h_{dr}^{\downarrow} \\ & & & & E_{r\uparrow}+g_rP_{rz} & g_r\Big(P_{rx}+iP_{ry}\Big) \\ & & & & & E_{r\downarrow}-g_rP_{rz} \end{pmatrix}$$

The energy of the left contact for spin-up (spin-down) carriers is $E_{l\uparrow}$ ($E_{l\downarrow}$), the energy of the defect for spin-up (spin-down) carriers is $E_{d\uparrow}$ ($E_{d\downarrow}$), and the energy of the right contact for spin-up (spin-down) carriers is $E_{r\uparrow}$ ($E_{r\downarrow}$). The Landé g factors of the left and right contacts and the defect are g_l, g_r, and g_d, respectively. The spin polarization of the left and right contacts is P_l and P_r, respectively. The angle of the spin polarization with $\hat{z}$ for the left and right contacts is θ_l and θ_r, respectively. The external magnetic field is $B = \{B_x, B_y, B_z\}$. We assume a sufficient coercive field to fix the spin polarization of the defects unchanged in this applied magnetic field. The h matrix elements represent the coherent hopping of the carriers that conserve spin. The h's have the same role as T_{mkn}, except that they are spin-dependent and for a fixed k.

The jump operators govern the evolution of the density matrix and determine the steady-state solution. In this formalism, the list of jump operators that preserve spin and introduce decoherence and current into the system are

$$\begin{aligned} L_{ld}^{\uparrow} &= \sqrt{\gamma_{ld}^{\uparrow} cos\Big(\frac{\theta_l}{2}\Big)}\, c_{l\uparrow} d_{\uparrow}^{\dagger} \\ L_{ld}^{\downarrow} &= \sqrt{\gamma_{ld}^{\downarrow} sin\Big(\frac{\theta_l}{2}\Big)}\, c_{l\downarrow} d_{\downarrow}^{\dagger} \\ L_{dr}^{\uparrow} &= \sqrt{\gamma_{dr}^{\uparrow} cos\Big(\frac{\theta_r}{2}\Big)}\, d_{\uparrow} c_{r\uparrow}^{\dagger} \\ L_{dr}^{\downarrow} &= \sqrt{\gamma_{dr}^{\downarrow} sin\Big(\frac{\theta_r}{2}\Big)}\, d_{\downarrow} c_{r\downarrow}^{\dagger} \end{aligned} \tag{10}$$

The right moving current operator is

$$\begin{aligned} \hat{I}_r &= \hat{I}_{r\uparrow} + \hat{I}_{r\downarrow} \\ \hat{I}_{r\uparrow} &= \frac{ei h_{dr}^{\uparrow}}{\hbar}\big(d_{\uparrow} c_{r\uparrow}^{\dagger} - c_{r\uparrow} d_{\uparrow}^{\dagger}\big) \\ \hat{I}_{r\downarrow} &= \frac{ei h_{dr}^{\downarrow}}{\hbar}\big(d_{\downarrow} c_{r\downarrow}^{\dagger} - c_{r\downarrow} d_{\downarrow}^{\dagger}\big) \end{aligned} \tag{11}$$

According to Eq. (6), the current is:

$$\begin{aligned} I_{r\uparrow} &= \left(-2\frac{e h_{dr}^{\uparrow}}{\hbar}\right) \mathfrak{Im}\left(\rho_{d\uparrow r\uparrow}^{ss}\right) \\ I_{r\downarrow} &= \left(-2\frac{e h_{dr}^{\downarrow}}{\hbar}\right) \mathfrak{Im}\left(\rho_{d\downarrow r\downarrow}^{ss}\right) \end{aligned} \tag{12}$$

where $\mathfrak{Im}$ is the imaginary part of the specified ρ^{ss} element.

We are interested in the spin relaxation time (T_1) of nonequilibrium spin-up and spin-down polarizations at the defect, as well as the decoherence time (T_2); these can be extracted from the time evolution of the density matrix. To obtain these we fit the corresponding density matrix element to

$$f = p_m^{ss} + f_o e^{f_1 t} \sin(f_2 t + f_3), \tag{13}$$

where f_o, f_1, f_2, and f_3 are fit parameters. The absolute value of f_1 is the same as Γ_m, the decay time of matrix element m. We are interested in $m = d\uparrow d\uparrow$, $m = d\downarrow d\downarrow$, and $m = d\uparrow d\downarrow$, which correspond to T_1 of spin-up, T_1 of spin-down, and T_2 of the carrier at the defect.

III. RESULTS

A. Modeling different materials

Some parameters describe the general properties of the host material and the defect. It is instructive to see how these parameters affect the total current without a magnetic field or polarized contacts.

The Hamiltonian that governs the evolution of the system has hopping parameters as its off diagonal elements, $h_{ld}^{\uparrow}$, $h_{ld}^{\downarrow}$, $h_{dr}^{\uparrow}$, and $h_{dr}^{\downarrow}$. These constants are not necessarily the same and take different values for different systems. To study their impact on the total current, we first consider the case where they are all equal. If one wants to model a real experiment with this Hamiltonian, these parameters must be chosen carefully. We assume they are on the order of a few microamperes, which are converted to a hopping rate by dividing by the number of Coulombs per electron (C), then converted to energy units (eV) by multiplying by $\hbar$ in units of eV·s. For the sake of comparison, we define a dimensionless hopping constant, h as follows,

$$\frac{\hbar}{\mathrm{C}} h = h_{ld}^{\uparrow} = h_{ld}^{\downarrow} = h_{dr}^{\uparrow} = h_{dr}^{\downarrow} \tag{14}$$

Fig. 2 shows how the hopping constant affects the total current as a function of the energy of the defect. In this example, the energy of the left (right) contact is fixed at 15 eV (10 eV) at zero temperature. The energy levels

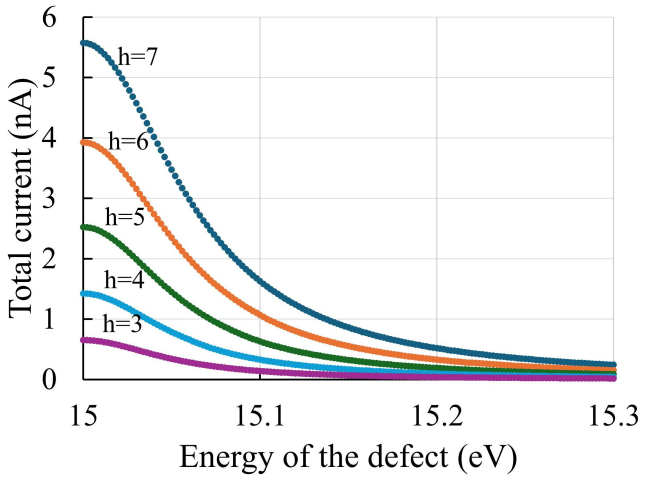

FIG. 2. Dependence of total current on the hopping constant in the absence of an external magnetic field and with unpolarized contacts.

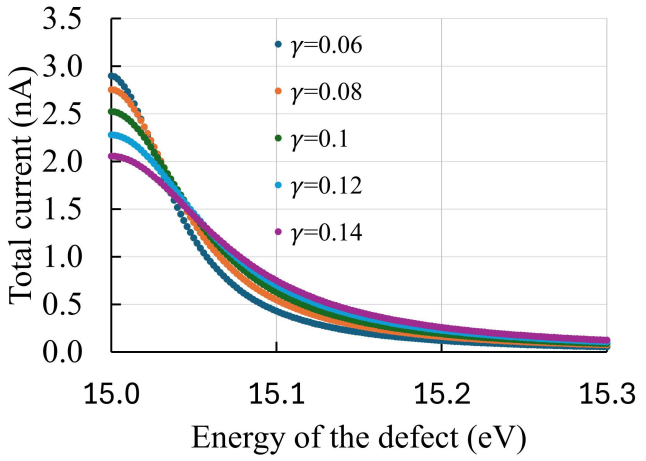

FIG. 3. Dependence of the total current on the jump parameters in the absence of an external magnetic field and with unpolarized contacts.

of the contact can be altered by applying voltage. The current drops exponentially when the energy of the defect is higher than that of the left contact. This shows that if we change the energy levels by applying the magnetic field, a small change in the energy level causes a greater change in the current. In our example, we choose $h = 5$.

Another set of parameters that captures the properties of the materials is the jump parameters: $\gamma_{ld}^{\uparrow}$, $\gamma_{ld}^{\downarrow}$,$\gamma_{dr}^{\uparrow}$, and $\gamma_{dr}^{\downarrow}$. The effect of the jump parameters on current differs from that of the hopping constant, as shown in Fig. 3. For lower values of the jump parameters, the current drops more rapidly. In our example, we assume all the jump parameters are the same, and we denote them by $\gamma = 0.1$. Adjusting these parameters can be used to simulate spin blockade. However, in the next section, we show that the spin blockade can also be identified when all of these parameters are the same.

FIG. 4. Spin blockade with one polarized contact and its dependence on magnetic field.

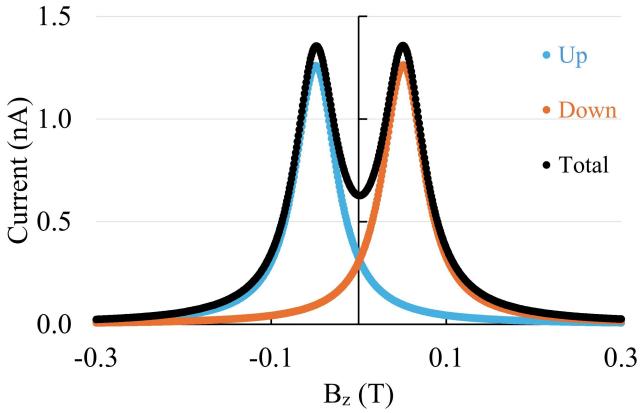

B. Spin blockade

Although the spin blockade can be manipulated by spin dependent interaction between the carriers and the defect environment, one can modify the spin blockade also by changing the applied magnetic field even when all other parameters are equal. An external magnetic field shifts the energy levels of the spin-up and spin-down carriers differently, and in the cotunneling region the resulting change in current due to this energy shift is significant. Thus current in the cotunneling regime is much more sensitive to the applied magnetic field than in sequential tunneling. Fig. III B shows how spin blockade can be achieved even when all the hopping constants are set to 5 and the jump parameters are 0.1. In this example, the defect's energy level in the absence of a magnetic field is 15.1 eV, which is 0.1 eV higher than that of the left contact. The left contact is magnetized to 1 mT in the $\hat{z}$ direction, and the right contact is not magnetized. The applied magnetic field acting on the defect is also in the $\hat{z}$ direction. When the magnetic field is applied to the defect, the energy level of the spin-down state is lowered, and the energy of the spin-up state increases. This slight change in the spin energy levels results in a dramatic change in current because the defect is in the cotunneling region.

Another interesting example is shown in Fig. 5. In this case, the left contact has the same polarization as before, and the right contact is polarized in the $\hat{x}$ direction. The applied magnetic field has a constant magnitude but changes direction in the yz plane, parameterized by the angle θ. We can tune the strength of the magnetic field such that the spin-down current is higher than the spin-up current only within a very narrow range of angles.

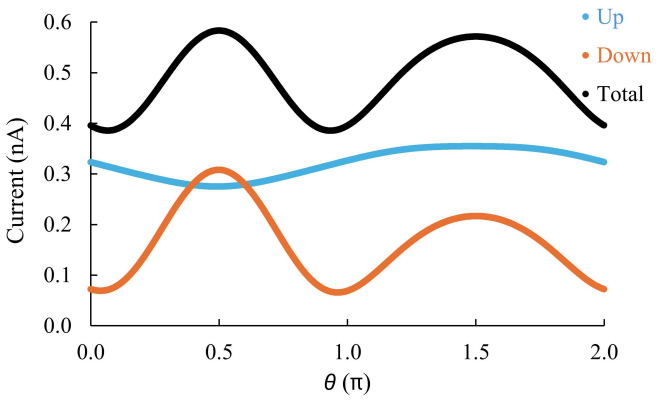

FIG. 5. Spin blockade from rotating the magnetic field in the yz plane when both contacts are magnetized.

C. Decoherence and dephasing

The decoherence of the spin-up and spin-down states and the dephasing time are also functions of the applied magnetic field. In order to calculate these time scales, we fit the time evolution of the density matrix element of interest to Eq. (13). As discussed earlier, f_1 is equivalent to the decay constant of the matrix element of interest, m, as shown in Fig. 6. For an applied magnetic field of 0.1 T (and 0.2 T), the T_1 relaxation times for the spin-up and spin-down states on the defect are 118.11 s (118.08 s) and 140.7235 s (129.932167 s), respectively. Additionally, the dephasing time (T_2) of the defect is 269.7866 s (487.836 s).

IV. CONCLUSION

We have developed a model to describe current in the cotunneling regime within the Markovian approximation in the presence of an external magnetic field and spin polarized contacts. The model contains a few free parameters to describe different host materials and defects. More defects of different types can be added to the model by increasing the dimension of the Hamiltonian. We have looked at a simple model to study the effect of various parameters on the current. Time evolution of the density matrix was presented, which was used to extract T_1 and T_2.

V. ACKNOWLEDGMENTS

Research primarily supported as part of the Center for Energy Efficient Magnonics, an Energy Frontier Research Center funded by the US Department of Energy (DOE), Office of Science, Office of Basic Energy Sciences (BES) under Award No. DE-AC02-76SF00515; initial setup of the formalism was supported by the National Science Foundation (NSF) QII-TAQS under award number OMA-1936219.

a)

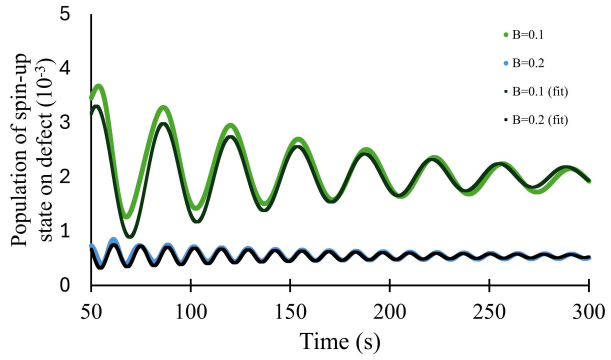

b)

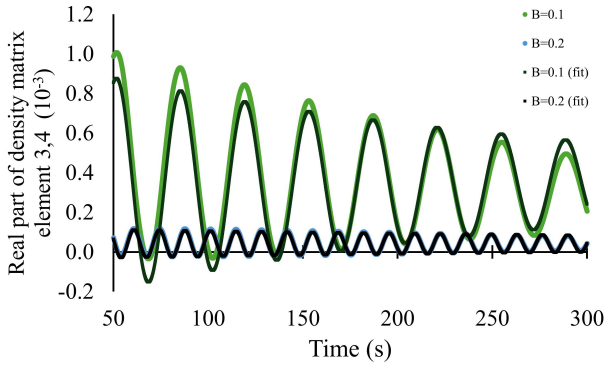

c)

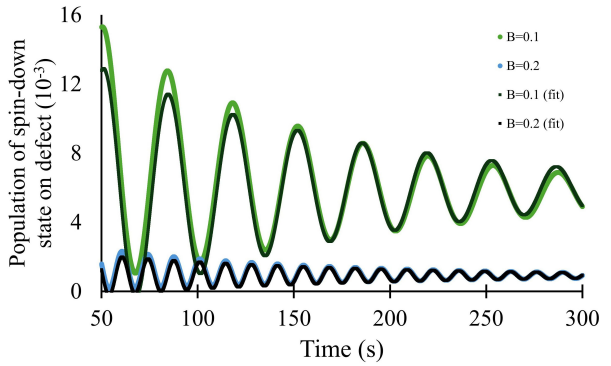

FIG. 6. Time evolution of specific density matrix elements for various magnetic fields. Green (blue) lines correspond to 0.1 T (0.2 T), and the black lines represent the fit from Eq. (13). a) Density matrix $\rho_{3,3}$, corresponding to the spin-up state on the defect. b) Real part of density matrix $\rho_{3,4}$, which corresponds to the dephasing time of the carrier on the defect. c) Density matrix $\rho_{4,4}$, corresponding to the spin-down state on the defect.

[1] D. D. Awschalom, N. Samarth, and D. Loss, eds., *Semiconductor Spintronics and Quantum Computation* (Springer Verlag, Heidelberg, 2002).

[2] S. A. Wolf, D. D. Awschalom, R. A. Buhrman, J. M. Daughton, S. von Molnár, M. L. Roukes, A. Y. Chtchelkanova, and D. M. Treger, Spintronics: A spin-based electronics vision for the future, Science **294**, 1488 (2001).

[3] A. Fert, Nobel lecture: Origin, development, and future of spintronics, Rev. Mod. Phys. **80**, 1517 (2008).

[4] P. A. Grünberg, Nobel lecture: From spin waves to giant magnetoresistance and beyond, Rev. Mod. Phys. **80**, 1531 (2008).

[5] D. C. Worledge, C. Safranski, G. Hu, J. Z. Sun, P. Hashemi, S. L. Brown, L. Buzi, C. P. D'Emic, M. G. Gottwald, O. Gunawan, H. Jung, S. Karimeddiny, J. Kim, and P. L. Trouilloud, Stt-mram - status and outlook, in *2022 IEEE 33rd Magnetic Recording Conference (TMRC)* (2022) pp. 1–2.

[6] A. Fert and F. N. Van Dau, Spintronics, from giant magnetoresistance to magnetic skyrmions and topological insulators, Comptes Rendus Physique **20**, 817 (2019).

[7] D.-F. Shao and E. Y. Tsymbal, Antiferromagnetic tunnel junctions for spintronics, npj Spintronics **2**, 13 (2024).

[8] L. Han, X. Luo, Y. Xu, H. Bai, W. Zhu, Y. Zhu, G. Yu, C. Song, and F. Pan, Electrical-controllable antiferromagnet-based tunnel junction, Nano Letters **24**, 4165 (2024).

[9] Y. Shao and P. Khalili Amiri, Progress and application perspectives of voltage-controlled magnetic tunnel junctions, Advanced Materials Technologies **8**, 2300676 (2023).

[10] K. Samanta, Y.-Y. Jiang, T. R. Paudel, D.-F. Shao, and E. Y. Tsymbal, Tunneling magnetoresistance in magnetic tunnel junctions with a single ferromagnetic electrode, Phys. Rev. B **109**, 174407 (2024).

[11] R. Hanson, L. P. Kouwenhoven, J. R. Petta, S. Tarucha, and L. M. K. Vandersypen, Spins in few-electron quantum dots, Rev. Mod. Phys. **79**, 1217 (2007).

[12] Y. Song and H. Dery, Magnetic-field-modulated resonant tunneling in ferromagnetic-insulator-nonmagnetic junctions, Phys. Rev. Lett. **113**, 047205 (2014).

[13] O. Txoperena, Y. Song, L. Qing, M. Gobbi, L. E. Hueso, H. Dery, and F. Casanova, Impurity-assisted tunneling magnetoresistance under a weak magnetic field, Phys. Rev. Lett. **113**, 146601 (2014).

[14] H. Inoue, A. G. Swartz, N. J. Harmon, T. Tachikawa, Y. Hikita, M. E. Flatté, and H. Y. Hwang, Origin of the magnetoresistance in oxide tunnel junctions determined through electric polarization control of the interface, Phys. Rev. X **5**, 041023 (2015).

[15] N. J. Harmon and M. E. Flatté, Theory of oblique-field magnetoresistance from spin centers in three-terminal spintronic devices, Phys. Rev. B **103**, 035310 (2021).

[16] C. J. Cochrane and P. M. Lenahan, Zero-field detection of spin dependent recombination with direct observation of electron nuclear hyperfine interactions in the absence of an oscillating electromagnetic field, J. Appl. Phys. **112**, 123714 (2012).

[17] N. J. Harmon, J. P. Ashton, P. M. Lenahan, and M. E. Flatté, Spin-dependent capture mechanism for magnetic field effects on interface recombination current in semiconductor devices, Applied Physics Letters **123**, 251603 (2023).

[18] S. J. Moxim, N. J. Harmon, K. J. Myers, J. P. Ashton, E. B. Frantz, M. E. Flatté, P. M. Lenahan, and J. T. Ryan, Tunable zero-field magnetoresistance responses in si transistors: Origins and applications, Journal of Applied Physics **135**, 155703 (2024).

[19] C. J. Cochrane, J. Blacksberg, M. A. Anders, and P. M. Lenahan, Vectorized magnetometer for space applications using electrical readout of atomic scale defects in silicon carbide, Scientific Reports **6**, 37077 (2016).

[20] S. Kovarik, R. Schlitz, A. Vishwakarma, D. Ruckert, P. Gambardella, and S. Stepanow, Spin torque driven electron paramagnetic resonance of a single spin in a pentacene molecule, Science **384**, 1368 (2024).

[21] S. R. McMillan, N. J. Harmon, and M. E. Flatté, Image of dynamic local exchange interactions in the dc magnetoresistance of spin-polarized current through a dopant, Phys. Rev. Lett. **125**, 257203 (2020).

[22] N. J. Harmon and M. E. Flatté, Theory of spin-coherent electrical transport through a defect spin state in a metal/insulator/ferromagnet tunnel junction undergoing ferromagnetic resonance, Phys. Rev. B **98**, 035412 (2018).

[23] Y. V. Nazarov, Quantum noise in mesoscopic physics (Springer Dordrecht, 2003) pp. 149,172.

[24] A. Cottet, W. Belzig, and C. Bruder, Positive cross-correlations due to dynamical channel blockade in a three-terminal quantum dot, Phys. Rev. B **70**, 115315 (2004).

[25] F. M. Souza, J. C. Egues, and A. P. Jauho, Quantum dot as a spin-current diode: A master-equation approach, Phys. Rev. B **75**, 165303 (2007).

[26] C. A. Merchant and N. Marković, Current and shot noise measurements in a carbon nanotube-based spin diode (invited), Journal of Applied Physics **105**, 07C711 (2009).

[27] D. Loss and E. V. Sukhorukov, Probing entanglement and nonlocality of electrons in a double-dot via transport and noise, Phys. Rev. Lett. **84**, 1035 (2000).

[28] M. Kavand, Z. Phillips, W. H. Koll, M. Hamilton, E. Perez-Hoyos, R. Greer, F. Ara, D. Pharis, K. Maleki, M. Xu, *et al.*, A general and modular approach to solid-state integration and readout of zero-dimensional quantum systems, arXiv preprint arXiv:2407.11189 (2025).